Marine Pollution Bulletin 222 (2026) 118815

Contents lists available at ScienceDirect

Marine Pollution Bulletin

journal homepage: www.elsevier.com/locate/marpolbul

Color disparity enhances the toxic effects of polystyrene microplastics on *Cladocopium goreaui*

Tianyi Niu [a,c,d], Yating Yang [a], Sanqiang Gong [a], Kefu Yu [a,b], Jiayuan Liang [a,*]

[a] Guangxi Laboratory on the Study of Coral Reefs in the South China Sea, School of Marine Sciences, Guangxi University, Nanning, 530004, China
[b] Southern Marine Science and Engineering Guangdong Laboratory (Guangzhou), Guangzhou, 510030, China
[c] State Key Laboratory of Urban and Regional Ecology, Research Center for Eco-Environmental Sciences, Chinese Academy of Sciences, Beijing, 100085, China
[d] University of Chinese Academy of Sciences, Beijing, 100049, China

ARTICLE INFO

Keywords:
Coral reef ecosystems
Symbiodiniaceae
Microplastic color disparity
Biosynthesis inhibition
Metabolic disruption

ABSTRACT

Coral reef ecosystems are increasingly threatened by environmental stressors, with microplastics (MPs) emerging as a pervasive and harmful contaminant. As essential symbionts of reef-building corals, *Symbiodiniaceae* are vital to coral health; however, their physiological responses to MPs remain largely unexplored. This study investigates the toxic effects of polystyrene microplastics (PS-MPs) of five distinct colors (red, yellow, green, blue, and white) on *Cladocopium goreaui*, a dominant coral symbiont. Exposure to 5 μm PS-MPs at 20 mg/L significantly inhibited algal growth, with blue and white PS-MPs exhibiting the strongest suppression. Growth rates decreased by up to approximately 36.0 % compared to controls over a 20-day exposure period. Although *C. goreaui* upregulated photosynthetic pigment content to compensate for reduced light availability due to MP aggregation, a substantial portion of the generated energy was diverted to mitigate oxidative stress. Transcriptomic analysis revealed that PS-MPs exposure downregulated key genes involved in biosynthetic pathways (e.g., peptide/amide formation) and primary metabolism (e.g., nitrogen assimilation, lipid metabolism). The pronounced toxicity of blue and white PS-MPs was attributed to their strong suppression of fatty acid metabolism and ribosomal function. These findings highlight the role of color disparity in modulating MP toxicity and offer new insight into the physiological and molecular responses of coral symbionts to MP pollution, with implications for coral reef health and resilience.

1. Introduction

Most coral reefs are distributed in tropical and subtropical oligotrophic shallow waters. Despite covering only approximately 0.25 % of the global ocean area, these ecosystems hold immense ecological and economic significance for humanity. Renowned as the "tropical rainforests of the sea", coral reefs support extraordinary biodiversity and functional diversity while providing critical habitat for nearly 30 % of marine species. Their unique combination of ecological value, aesthetic appeal, and ecosystem services makes them indispensable to marine environments and human societies alike (Reaka-Kudla, 1997; Yu, 2018; Jones et al., 2022). The unique morphological structure of coral reefs enables them to function as natural hydraulic barriers These ecosystems serve three critical coastal protection roles: (1) replenishing beach sand through biogenic sediment production, (2) filtering and trapping suspended sediments, and (3) significantly mitigating shoreline erosion through wave energy dissipation (Smith, 1978; Fisher et al., 2015; Peixoto et al., 2019; Woodhead et al., 2019). Coral holobionts comprise the coral host's mucus, ambient seawater, and sediment-associated benthic microbial communities (Pogoreutz et al., 2020). The composition and structure of microbial communities within coral holobionts are highly responsive to environmental fluctuations (e.g., temperature, light availability) and stressors (e.g., toxic substances) (Ursell et al., 2012; Webster and Thomas, 2016). The symbiotic relationship between *Symbiodiniaceae* and reef-building corals forms the foundation of coral reef ecosystems, with the photosynthates (e.g., amino acids, glucose, glycerol) provided by the algae satisfying up to 90 % of the coral hosts' energy requirements (Houlbrèque and Ferrier-Pagès, 2009; González-Pech et al., 2019). *C. goreaui* forms widespread symbiotic relationships with corals across the Indo-Pacific region, exhibiting high photosynthetic efficiency that enhances host coral tolerance to seasonal low temperatures and elevated nutrient conditions (Baker et al., 2013).

* Corresponding author.
E-mail address: jyliang@gxu.edu.cn (J. Liang).

https://doi.org/10.1016/j.marpolbul.2025.118815
Received 16 July 2025; Received in revised form 31 August 2025; Accepted 5 October 2025
Available online 8 October 2025

Subject to escalating pressures from global warming, overfishing, and environmental pollution, coral reef ecosystems are experiencing accelerating degradation (Hughes et al., 2003; van Woesik and Kratochwill, 2022). Coral bleaching has emerged as the predominant driver of large-scale reef degradation worldwide. The dazzling colors of corals come from *Symbiodiniaceae* living in their tissues and when corals lose these *Symbiodiniaceae* or the *Symbiodiniaceae* loss of pigmentation, the corals turn white—a process called bleaching (Guibert, 2024; Mellin et al., 2024). Mortality occurs in bleached corals when *Symbiodiniaceae* repopulation does not achieve threshold densities within species-specific recovery windows.

Given the ecological fragility of coral reefs and their dependence on *Symbiodiniaceae*, it is crucial to understand emerging anthropogenic stressors that may exacerbate reef degradation. Among these, plastic pollution and particularly MPs have attracted increasing global attention. Anthropogenic development has made plastics and their additives a major emerging threat to Earth's ecosystems (Jambeck et al., 2015; Sendra et al., 2021). Under environmental stressors including photodegradation (UV exposure), oxidative weathering, and microbial degradation, plastics undergo progressive fragmentation into microscale particles (Thompson et al., 2004; Lambert et al., 2013; Jambeck et al., 2015; Auta et al., 2017). MPs are globally pervasive, found in rivers, soils, oceans, and air (Li et al., 2021a; Zhou et al., 2021). Each year, over 100,000 tons of plastic enter the oceans through various pathways, where they are carried by ocean currents, widely dispersed, and pose serious threats to marine ecosystems across entire food webs (Liu et al., 2022; Xia et al., 2023; Zhang et al., 2024; Kazancı et al., 2025). MP ingestion by marine organisms has become ubiquitous, raising significant concerns about ecosystem stability (Kühn and Van Franeker, 2020; Lu et al., 2025). These MPs cause severe physiological impacts, including gastrointestinal obstruction, organ damage, and growth impairment (Wright et al., 2013; Huang et al., 2019). A MP analysis of 1381 fish specimens revealed contamination in 42.4 % of samples, comprising fibers, microbeads, and fragments (Peters et al., 2017). Importantly, the ecological risks of MPs are not limited to higher trophic levels such as fish, but also extend to primary producers like marine algae, which play key roles in sustaining coral reef ecosystems. MPs pose significant threats to marine algae, causing both direct physical damage and photosynthetic inhibition (Ding et al., 2019b). Elevated MP concentrations inhibit algal growth, induce oxidative stress, and enhance the release of algal proteins and polysaccharides (Li et al., 2020). These MPs can form aggregates with the secreted biomolecules, which subsequently persist in the water column or settle into benthic sediments (Lagarde et al., 2016; Zhang et al., 2017; Li et al., 2020; Li et al., 2021b).

Building on this, recent studies have suggested that not only the presence of MPs but also their physical characteristics—such as size, shape, and particularly color—can further modulate their ecological impacts. In natural environments, coloration is an evolutionarily adaptive trait that enhances survival through predator avoidance or light capture optimization (Croce and Van Amerongen, 2014; Karpestam et al., 2014). Color is a functional trait in both natural and synthetic systems. Plastics are manufactured in various colors to fulfill specific industrial purposes, with color influencing their environmental interactions (Shtykova et al., 2006; Greenway and Gerstenberger, 2010). Colored MPs dominate aquatic plastic debris, with black, white, red, yellow, green, and blue being most common (Shaw and Day, 1994; Su et al., 2016; Wang et al., 2017; Zhang et al., 2018). A global survey of oceanic floating plastic fragments revealed that white and transparent/sem-transparent MPs are the most abundant, accounting for up to 47 % of particles collected, highlighting the environmental relevance of chromatic variation in MPs (Zhao et al., 2022). The plastisphere refers to the unique ecological niche formed by microbial communities adhering to and colonizing MP surfaces (Zettler et al., 2013). Blue polyethylene MPs (2.76–2.88 mm) uniquely enhance microbial diversity and select for distinct taxa in aquaculture pond plastispheres compared to yellow/transparent counterparts (Wen et al., 2020), possibly because different colors alter surface energy and adsorption properties, thereby shaping microbial colonization dynamics. Exposure to 5 μm PS-MPs of varying colors (white, green, orange, red) significantly inhibited growth in the freshwater microalga *Scenedesmus obliquus*, with the least suppression observed in green PS-MPs that closely matched the algal cell's pigmentation (Chen et al., 2020). This pattern suggests that color-dependent light absorbance and reflectance can influence photosynthetically active radiation, thereby modulating algal physiological responses. In addition, recent studies have demonstrated that marine and freshwater organisms, including fish and crustaceans, exhibit selective ingestion based on MP color, suggesting ecological relevance of plastic color in exposure dynamics and potential toxicity (Horie et al., 2024). Such feeding selectivity may reflect visual perception biases, where certain colors mimic natural prey or contrast strongly with the surrounding environment, thereby altering ingestion risk. These findings indicate color-mediated differential ecological risks of MPs, though the mechanistic basis of chromatic toxicity is poorly understood.

Reef-building corals serve as the ecological foundation of coral reef ecosystems, predominantly establishing symbiotic relationships with *Symbiodiniaceae* through horizontal transmission. This coral-algal symbiosis represents a critical biological partnership, where the physiological status of the symbionts directly determines holobiont stability. In recent years, escalating inputs of MPs into marine environments have emerged as a significant threat to *Symbiodiniaceae* survival, consequently compromising the functionality of coral reef ecosystems. PS-MPs, due to their persistence and bioavailability, exhibit high mobility in the environment, can accumulate through food chains, and induce multiple biological toxic effects such as cytotoxicity and oxidative stress, thereby posing a serious threat to ecosystems (Wang et al., 2024; Wang et al., 2025).

To elucidate the color-dependent mechanisms of MP toxicity in *Symbiodiniaceae*, we investigated the responses of the globally widespread coral symbiont *C. goreaui* to five color-annotated PS-MPs (red, yellow, green, blue, and white; 20 mg/L; 5 μm). By systematically assessing algal growth rate, photosynthetic efficiency, oxidative stress responses, and transcriptomic alterations, this study reveals color-specific impacts of PS-MPs on cellular physiology and gene expression. Our findings demonstrate that PS-MPs of different colors exert distinct levels of toxicity on *Symbiodiniaceae*, highlight the molecular mechanisms driving these divergent responses, and provide a basis for more accurate risk assessment of color-dependent MP impacts on coral–algal symbioses and reef conservation.

2. Materials and methods

2.1. Materials and experimental design

The strain of *C. goreaui* used in this study was isolated by our laboratory from *Acropora pruinosa* collected in Weizhou Island, Beibu Gulf, South China Sea (Qin et al., 2023). The cultures were maintained in L1 seawater medium under controlled conditions: salinity 35 ‰, temperature 25 ± 1 °C, light intensity 90 μmol photons m^{-2} s^{-1}, with a 14:10 h light: dark photoperiod (Guillard and Hargraves, 1993). L1 medium components were sourced from Guangyu Biotechnology Co., Ltd. (Shanghai, China). Monodisperse colored latex PS microspheres were obtained from Beisile Technology Research Center (Tianjin, China). These particles were synthesized by incorporating chromophores via surface coatings. The microspheres exhibit spherical morphology with smooth surfaces, high purity (>99 %), and narrow size distribution (5 μm ± 0.2 μm). In 250 mL conical flasks, *C. goreaui* was cultured in a 150 mL system until reaching a cell density of 1.0 × 10^5 cells/mL, after which PS-MPs stock solution was added to achieve a final concentration of 20 mg/L (Higher concentrations facilitate the observation of significant changes within a short period, enabling an effective assessment of the toxic effects arising from color differences in PS-MPs). In the control

group, an equal volume of ultrapure water (the solvent for the microplastics) was added. Six experimental treatments were established: red, yellow, green, blue, and white PS-MPs, along with a control group, each group with three biological replicates. All sampling procedures were conducted in a clean bench, and the experiment was maintained for 20 days.

2.2. Indicator measurement

2.2.1. growth ratios

At days 0, 5, 10, and 20 of the experiment, 1 mL aliquots were collected and fixed with 100 μL formaldehyde at 4 °C in the dark for 24 h. algal cells were then enumerated using a hemocytometer under an optical microscope. Cell density (cells/mL) and growth ratios were calculated from the recorded data. The specific growth rate (μ, day^{-1}) was determined as: $\mu = [\ln(N_2/N_1)] / (t_2 - t_1)$, where: N_1 and N_2 = cell densities (cells/mL) at time points t_1 and t_2, respectively.

2.2.2. Maximum photochemical efficiency Fv/fm and photosynthetic pigment content

Fv/fm was measured after 30-min dark adaptation using a PAM fluorometer (Walz, Germany) at four timepoints (days 0, 5, 10, 20). Measurements followed established protocols with 3 biological replicates (Schreiber et al., 1986; Sun, 2020). At each sampling timepoint (days 0, 5, 10, 20), 2 mL aliquots were centrifuged (5000 ×*g*, 5 min, 4 °C). The supernatant was discarded, and the pellet was resuspended in 1 mL methanol. After vortex mixing, samples were wrapped in aluminum foil and dark-incubated at 4 °C for 24 h to extract pigments. Following subsequent centrifugation (5000 ×*g*, 5 min, 4 °C), the supernatant was analyzed spectrophotometrically for optical density (OD) at 480, 510, 630, 664, and 750 nm wavelengths using a microplate reader (Ritchie, 2006). Light-protected protocols were strictly maintained throughout. Pigment contents were normalized to per-cell values and calculated as:

$$\text{Chlorophyll a } (\mu g/mL) = 13.6849 \times (OD_{664} - OD_{750}) - 3.4551 \times (OD_{630} - OD_{750})$$

$$\text{Chlorophyll c } (\mu g/mL) = -7.014 \times (OD_{664} - OD_{750}) + 32.9371 \times (OD_{630} - OD_{750})$$

$$\text{Carotenoids } (\mu g/mL) = 7.6 \times (OD_{480} - OD_{750}) - 1.49 \times (OD_{510} - OD_{750})$$

2.2.3. Extracellular polymeric substances content

Since the primary component of extracellular Polymeric Substances (EPS) is polysaccharides, EPS content was estimated by quantifying polysaccharide levels using the phenol-sulfuric acid (H_2SO_4) method (Li et al., 2020; Cao et al., 2022b; Yue et al., 2022). At days 0, 10, and 20 of the experiment, 5 mL of algal culture was heated at 80 °C for 30 min, followed by centrifugation at 8000 ×*g* and 4 °C for 10 min to collect the supernatant. Heat-extracted supernatants (80 °C, 30 min) were reacted with phenol/H_2SO_4 under controlled thermal conditions (100 °C × 20 min → 0 °C × 10 min). Absorbance at 490 nm was calibrated against glucose standards (0–90 μg/mL, $R^2 > 0.99$).

2.2.4. Soluble protein content, MDA level, and SOD activity

For cell lysis, at days 0, 10, and 20 of the experiment, 20 mL algal suspensions were pelleted (3000 ×g, 10 min, 4 °C), resuspended in PBS, and subjected to bead-beating (0.5 mm ZrO_2 beads; 10 s ON/30 s OFF ×6 cycles) in a pre-chilled homogenizer. Lysates were cleared by centrifugation (3000 ×*g*, 10 min, 4 °C). Total protein concentration in the supernatant was determined using a BCA microprotein assay kit (Sangon Biotech, Shanghai, China). Malondialdehyde (MDA) content was quantified with a commercial MDA assay kit (A003, Jiancheng Bioengineering, Nanjing, China). Superoxide dismutase (SOD) activity was measured using an SOD detection kit (A001, Jiancheng Bioengineering). All measurements were normalized to per-cell values.

2.3. Transcriptome sequencing

At the experimental endpoint (day 20), algal cells from 100 mL cultures were harvested by centrifugation (5000 ×*g*, 10 min, 4 °C). Following PBS washing (3 × 20 mL) and final pelleting, samples were snap-frozen in liquid nitrogen (30 min) prior to RNA-seq analysis (Illumina NovaSeq X Plus; Majorbio, Shanghai). Datasets were analyzed on the online platform of Majorbio Cloud Platform (https://cloud.majorbio.com/) (Han et al., 2024). The detailed steps are provided in the supplementary materials.

2.4. Statistical analysis

All statistical tests were implemented in SPSS. All data were tested for normality (Shapiro-Wilk test) and homogeneity of variances (Levene's test) prior to ANOVA. When these assumptions were satisfied, Tukey's HSD was applied for multiple comparisons ($p < 0.05$). Graphical representations were created in Origin, and all values expressed as mean ± SEM (n = X).

3. Results

3.1. PS-MPs exposure significantly inhibited the growth of C. goreaui

The decline in growth ratios directly reflected cellular damage in *C. goreaui*. All colored PS-MPs exposure significantly inhibited algal growth ($p < 0.05$), but the inhibition was less severe in color-matched groups (yellow and green) than in spectrally distinct groups (red, blue, and white) (Fig. 1A). Specifically, yellow and green PS-MPs caused transient growth inhibition during days 0–10, while red, blue, and white PS-MPs induced sustained suppression throughout the experiment. The most pronounced inhibition occurred in the blue and white groups, with growth rates decreasing by 33.6 % and 36 % (day 5), 32.5 % and 34.7 % (day 10), and 32.1 % and 35.4 % (day 20) compared to the control, respectively.

The photosynthesis of *Symbiodiniaceae* plays a very important role in symbiotic functional organisms. Throughout the experimental period, no significant changes in *Fv/fm* were observed across all treatment groups (Fig. 1B). As photosynthetic pigments are critical for maintaining photosynthetic function, exposure to 20 mg/L of 5 μm PS-MPs of different colors resulted in significantly increased chlorophyll *a* (Chl-a) content in the red, green, and blue groups compared to the control, except for the yellow and white groups (Fig. 1C). The red group exhibited the most pronounced increase in Chl-a at days 5–10 ($p < 0.001$). No significant difference in Chl-a content was detected between the yellow group and the control, while the white group showed a transient increase at day 5 ($p < 0.05$) followed by a significant decline at days 10–20 ($p < 0.05$). For chlorophyll *c* (Chl-c), the blue group demonstrated a highly significant increase ($p < 0.001$), whereas the yellow group showed a reduction at day 5 ($p < 0.05$) and the red group displayed elevated levels at days 10–20 ($p < 0.05$). The white group exhibited similar trends in Chl-c as in Chl-a (Fig. 1D). From days 5–20, carotenoid content significantly increased in the red and green groups ($p < 0.0001$), with the blue group showing a delayed response (significant only at day 20, $p < 0.001$). No significant change was observed in the yellow group, while the white group mirrored the Chl-a pattern (Fig. 1E).

3.2. PS-MPs exposure induced cellular damage in C. goreaui

EPS play a protective role against toxicant penetration into cells. Upon exposure to 20 mg/L of 5 μm color-differentiated PS-MPs, all groups exhibited significantly elevated EPS production by day 10 ($p <$

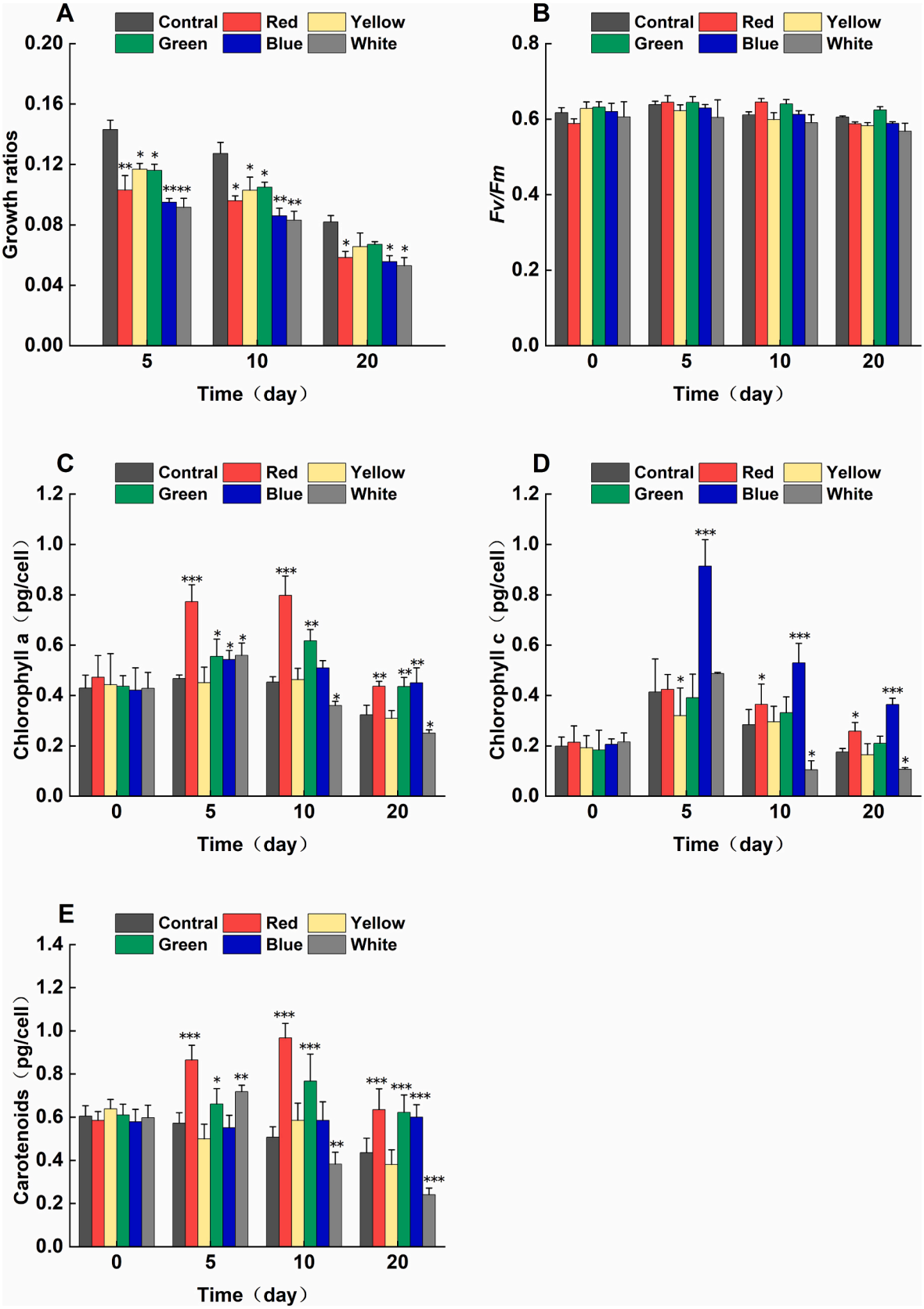

Fig. 1. The growth and photosynthetic indicators of *C. goreaui* after exposure to PS-MPs. (A) Growth ratios. (B) *Fv/fm*. (C) Chl-a content. (D) Chl-c content. (E) Carotenoids content. The bar shapes represent the mean ± the standard error (three biological replicates). The significance between the experimental group and the control group is indicated by asterisks (*: $p < 0.05$, **: $p < 0.01$, ***: $p < 0.001$).

0.001), with yellow and green groups (similar in color to algal cells) showing less pronounced increases than spectrally distinct red, blue, and white groups (Fig. 2A). The blue and white PS-MPs induced maximal EPS secretion, reaching 127 % and 139.9 % above control levels at day 10, and maintaining 83.7 % and 93.8 % increases at day 20, respectively.

Soluble proteins, serving as essential nutrients and osmoregulators, exhibited concentration patterns analogous to EPS following exposure to 20 mg/L of 5 μm color-variant PS-MPs. Consistent with EPS dynamics, yellow and green groups (spectrally similar to algal cells) demonstrated lower protein accumulation than red, blue, and white groups (Fig. 2B). All treatments showed significant increases in soluble protein content ($p < 0.05$), except the yellow group at day 10. Notably, blue and white PS-MPs triggered extreme upregulation ($p < 0.001$), elevating protein levels by 56.4 % and 82.3 % (day 10), and 114.1 % and 145.2 % (day 20) relative to controls, respectively.

MP toxicity induced substantial reactive oxygen species (ROS) generation in algal cells, where excessive ROS accumulation triggered membrane lipid peroxidation and elevated malondialdehyde (MDA) production. Superoxide dismutase (SOD) activity, as a critical ROS scavenger, showed coordinated patterns with MDA, extracellular polymeric substances (EPS), and soluble protein levels under 20 mg/L of 5 μm color-differentiated PS-MPs exposure (Figs. 2C, D). All treatments exhibited significant increases in both SOD activity and MDA content ($p < 0.05$), with yellow and green groups (spectrally matched to algal cells) displaying less pronounced responses than red, blue, and white groups. Specifically, blue and white PS-MPs induced the most severe oxidative stress: SOD activity surged to 58.3 % and 61.7 % above controls at day 10, and 113.7 % and 106 % at day 20, while MDA levels escalated by 94.6 % and 118.1 % (day 10), and 290.5 % and 313.1 % (day 20), respectively.

3.3. PS-MPs exposure suppressed biosynthesis and energy metabolism in *C. goreaui*

3.3.1. Gene expression and gene set level

Cluster analysis was performed using Pearson correlation coefficients with complete linkage clustering and Euclidean distance metrics, applying log10 transformation to group-averaged values. The results demonstrated high reproducibility across all biological replicates, with inter-sample correlation coefficients exceeding 0.97 (Fig. 3A). Principal component analysis (PCA) revealed distinct separation between blue/white PS-MPs groups and controls in terms of differentially expressed genes (DEGs) patterns (Fig. 3B). Raw counts were directly analyzed using DESeq2 based on the negative binomial distribution. Differentially expressed genes between groups were identified following standard normalization and filtering procedures, with default thresholds set at Padjust <0.05 and $|\log_2 FC| \geq 1$. Analysis of DEGs in *C. goreaui* following PS-MPs exposure showed that red, yellow, and green groups shared similar upregulated DEG profiles, whereas blue and white groups exhibited more extensive alterations, particularly the white group showing the greatest number of upregulated genes (Fig. 3C). For downregulated DEGs, the yellow group displayed the most substantial changes, followed by white, blue, green, and red groups in descending order.

Venn analysis of differentially expressed genes (DEGs) in *C. goreaui* following PS-MPs exposure revealed only 8 common DEGs across all five color groups, demonstrating distinct transcriptomic responses to different MP colors (Fig. 4A). Notably, blue and white PS-MPs, which showed the strongest growth inhibition, shared 465 overlapping DEGs. GO functional annotation (level 4) of these DEGs identified significant terms across three categories: Biological Process (BP), Cellular Component (CC), and Molecular Function (MF) (Fig. 4B). The most affected

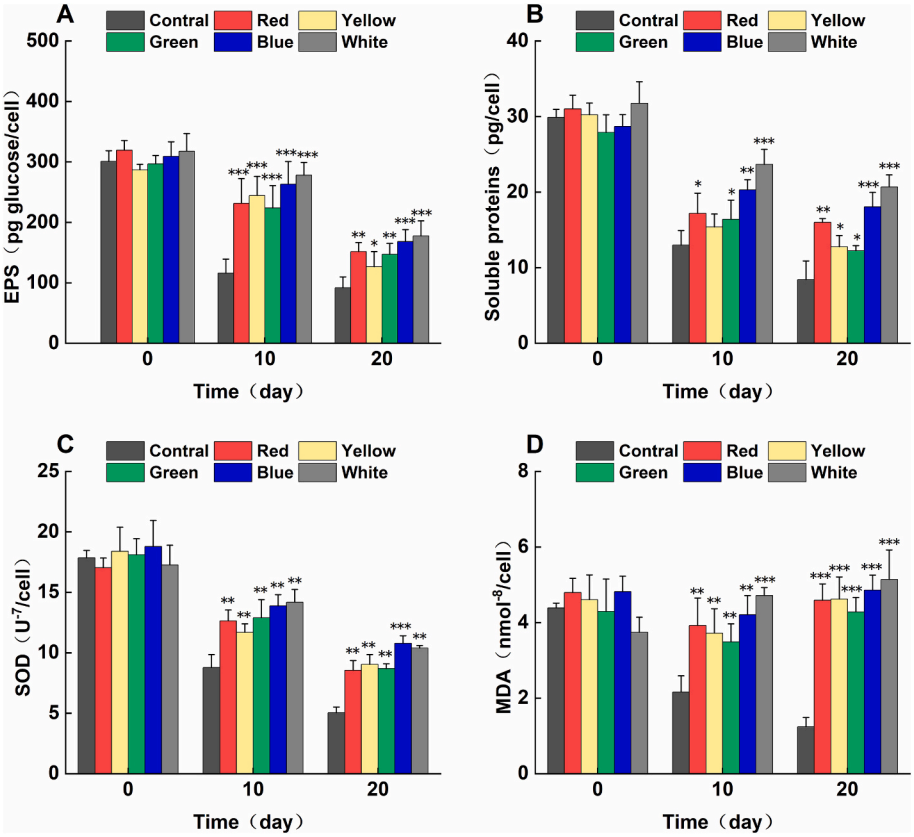

Fig. 2. The cellular defense and oxidative stress indicators of *C. goreaui* after exposure to PS-MPs. (A) EPS content. (B) soluble proteins content. (C) SOD activity. (D) MDA content. The bar shapes represent the mean ± the standard error (three biological replicates). The significance between the experimental group and the control group is indicated by asterisks (*: $p < 0.05$, **: $p < 0.01$, ***: $p < 0.001$).

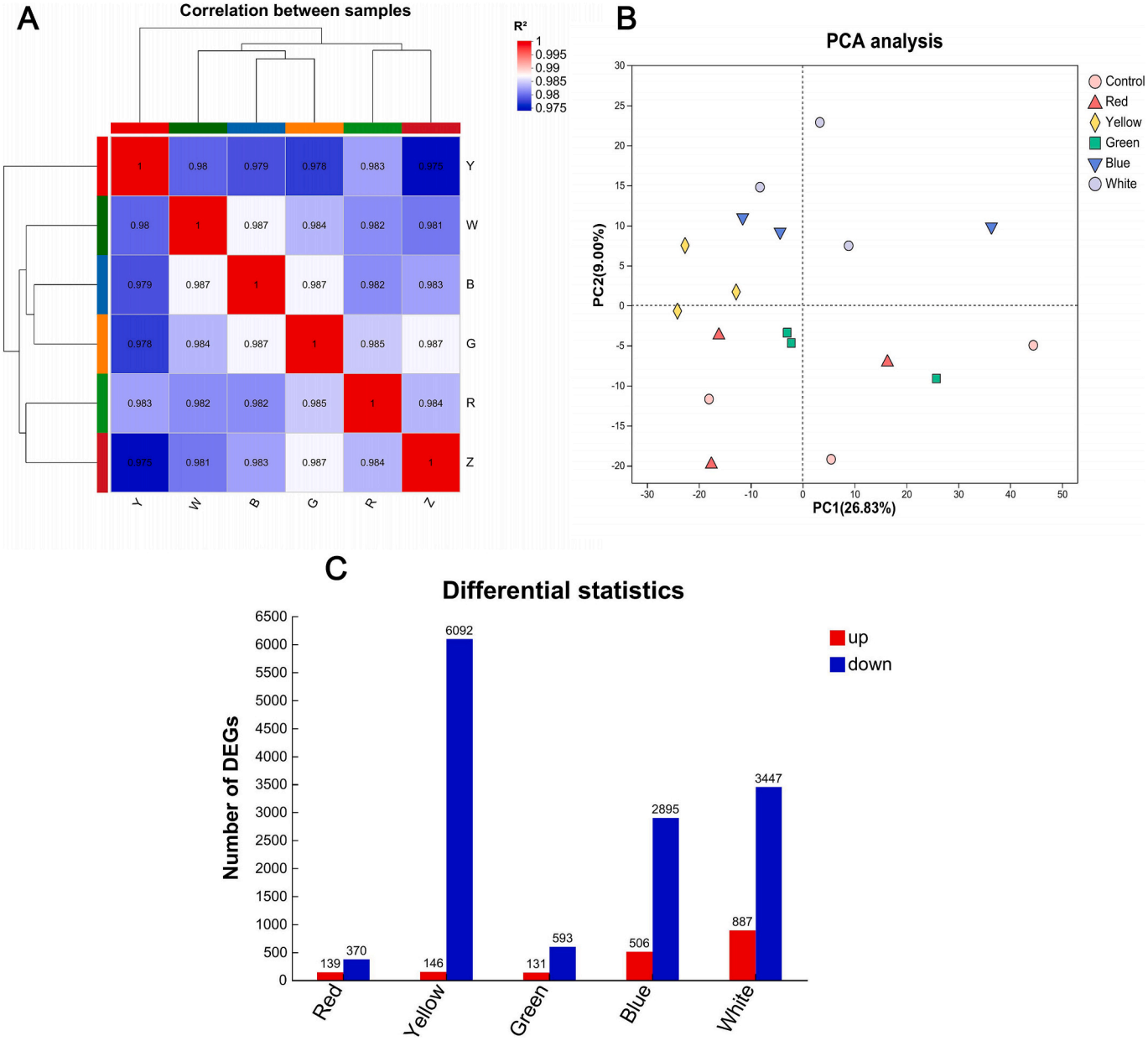

Fig. 3. Expression level analysis of genes in each group after exposure to PS-MPs. (A) Cluster analysis between samples. Z: Control; R: Red; Y: Yellow; G: Green; B: Blue; W: White. (B) PCA analysis between samples. (C) Differential expression statistics. Three biological replicates. (For interpretation of the references to color in this figure legend, the reader is referred to the web version of this article.)

molecular functions included ion binding, nucleotide binding, and ATP binding, while cellular processes were primarily associated with macromolecular metabolism and nitrogen/phosphorus metabolic pathways.

3.3.2. *Functional enrichment*

Protein-protein interaction (PPI) network analysis was conducted for the white PS-MPs group (showing strongest toxicity), from which 21 functionally pivotal genes were selected for cluster analysis, with results visualized in a heatmap (Fig. 5). These genes predominantly encode ribosomal proteins involved in large and small subunit assembly. Striking expression divergence was observed between the white group and controls, exhibiting inverse transcriptional patterns. Subsequent GO and KEGG enrichment analyses of differentially expressed genes (DEGs) across all groups were performed, with results displayed as the union of the top 10 most significantly enriched GO terms and KEGG pathways per group (Fig. 6).

GO enrichment analysis of DEGs revealed a spectral transition pattern following the color sequence from red to blue to white (Fig. 6A). Functional overlaps were observed specifically between white and blue groups, while blue groups additionally shared some terms with yellow groups. Red groups showed distinct GO profiles from all other treatments. Notably, the most growth-inhibitory groups (blue and white) exhibited significant suppression of ribosome-related functions, particularly cytoplasmic large ribosomal subunit assembly, protein-RNA complex organization, and protein-RNA complex assembly. Concurrently, blue and yellow groups showed impaired biosynthesis and metabolism of amides and peptides. Photosynthesis-related terms were downregulated in green groups, whereas red groups displayed reduced signal reception capacity for proteases.

Pathway analysis revealed consistent perturbations across multiple treatment groups in essential metabolic pathways including ribosome

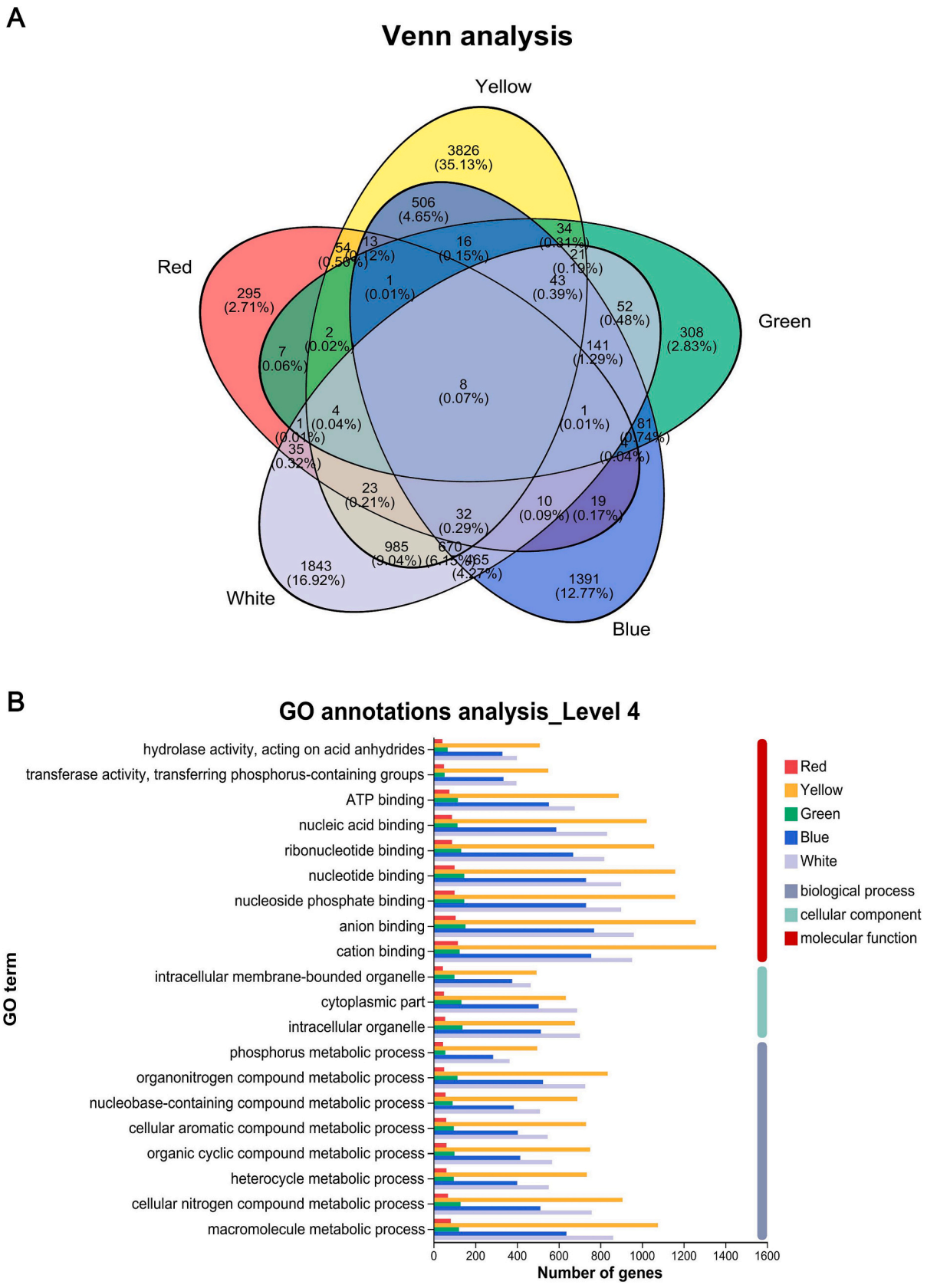

Fig. 4. Gene set analysis of DEGs in each group after exposure to PS-MPs. (A) Venn analysis of DEGs in each group. (B) GO functional annotation analysis. Three biological replicates.

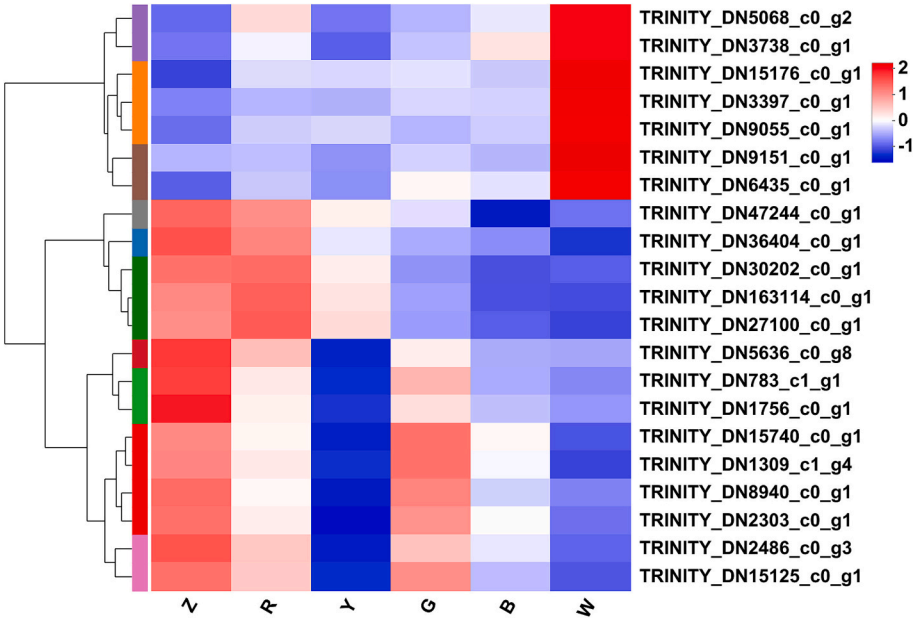

Fig. 5. DEGs clustering heatmap with strong importance after exposure to white PS-MPs. Z: Control; R: Red; Y: Yellow; G: Green; B: Blue; W: White. Three biological replicates. (For interpretation of the references to color in this figure legend, the reader is referred to the web version of this article.)

function, unsaturated fatty acid biosynthesis, TCA cycle, and lipoic acid metabolism (Fig. 6B) - all critical for cellular growth and proliferation in *C. goreaui*. The white group showed additional suppression of peroxisome and fatty acid degradation pathways, while the blue group exhibited impaired proteasome activity and endoplasmic reticulum protein processing. These findings indicate: (1) compromised energy metabolism and (2) attenuated proteolytic signaling in these high-toxicity groups. Furthermore, yellow groups displayed inhibited carbohydrate/alcohol biosynthesis and photosynthetic pathways, whereas red groups showed downregulation of sugar metabolism and disease resistance mechanisms - collectively suggesting severe impairment of energy production and stress defense capacities.

4. Discussion

4.1. PS-MPs exposure exerted detrimental effects on the growth of C. goreaui

The increasing severity of global coral reef degradation and the pivotal role of *Symbiodiniaceae* in reef ecosystems have driven growing research focus on their stress response mechanisms, with particular attention to MP toxicity as pollution escalates. Exposure to 1 μm PS-MPs at 5 mg/L concentration inhibited detoxification activity and assimilatory metabolism in *C. goreaui*, while activating ion transport mechanisms and elevating apoptosis levels, collectively suppressing algal growth (Su et al., 2020). In this study, 5 μm PS-MPs at 20 mg/L similarly reduced the growth ratios of *C. goreaui*, with greater growth inhibition observed in red, blue, and white groups that exhibited larger chromatic differences from algal cells compared to the spectrally similar yellow and green groups showing relatively milder suppression. This color-dependent toxicity likely reflects combined effects of optical shading and differential aggregation influencing cellular stress and transcriptional responses. Darker or more reflective colors may alter particle-cell adhesion rates, influencing aggregate formation and light penetration. This pattern was corroborated in parallel experiments with *Scenedesmus obliquus* exposed to 5 μm PS-MPs of different colors (red, orange, green, white), where the green PS-MPs (color-matched to chloroplasts) induced less toxicity than chromatic-mismatched groups, as further evidenced by irregular and slower algal cell motility in red, orange, and white treatments relative to green PS-MPs (Chen et al., 2020). Faster-moving algal cells can acquire greater light exposure, thereby generating higher biomass, suggesting potential color discrimination capabilities and chromatic preferences in these organisms. Previous studies have demonstrated that ultrastructural observations reveal adverse effects of MPs exposure on algal cells, including surface shrinkage and thylakoid distortion (Jiang et al., 2025; Liang et al., 2025). Furthermore, ribosomal function was severely impaired in all groups except the red treatment. Such ribosomal dysfunction may result from color-dependent aggregation and chemical interactions, as reflected in transcriptomic downregulation of ribosomal genes in blue and white groups (Ni and Buszczak, 2023). Ribosomal dysfunction induced by PS-MPs concurrently diminishes both antioxidant capacity (via enzyme activity reduction) and immune protease function, ultimately severely compromising *C. goreaui* growth, with the white group's uniquely elevated toxicity attributable to specific dysregulation of ribosomal subunit genes (60S/40S) (Ford et al., 2025).

For colors, Wen et al. demonstrated through biofilm cultivation experiments in aquaculture pond water systems with different colored MPs (blue, yellow, transparent) that plastisphere communities exhibited enhanced diversity and evenness, particularly in blue MP groups which harbored more unique species, indicating a color-driven selection mechanism among plastisphere microbiota (Wen et al., 2020). This finding is particularly relevant given that *Symbiodiniaceae* survival depends critically on symbiotic bacteria for essential nutrients like nitrogen and phosphorus. Previous studies have documented that PS-MPs tend to form large aggregates with *C. goreaui*, with these aggregates encapsulating significant populations of symbiotic bacteria within the plastisphere (Liang et al., 2025). Therefore, color-dependent aggregation may modulate light availability and bacterial interactions, potentially contributing to the observed growth variations and transcriptomic changes. Exposure to differently colored PS-MPs may induce distinct bacterial community shifts in the microalgal-bacterial symbiotic system, potentially contributing to the observed growth variations in *C. goreaui* across experimental groups. The chromatic properties of plastic microbeads, determined by wavelength-specific absorption and reflection patterns of surface dyes, critically influence light availability for photosynthesis. White PS-MPs, exhibiting poor light reflectivity, significantly reduced light energy acquisition in *C. goreaui*, leading to

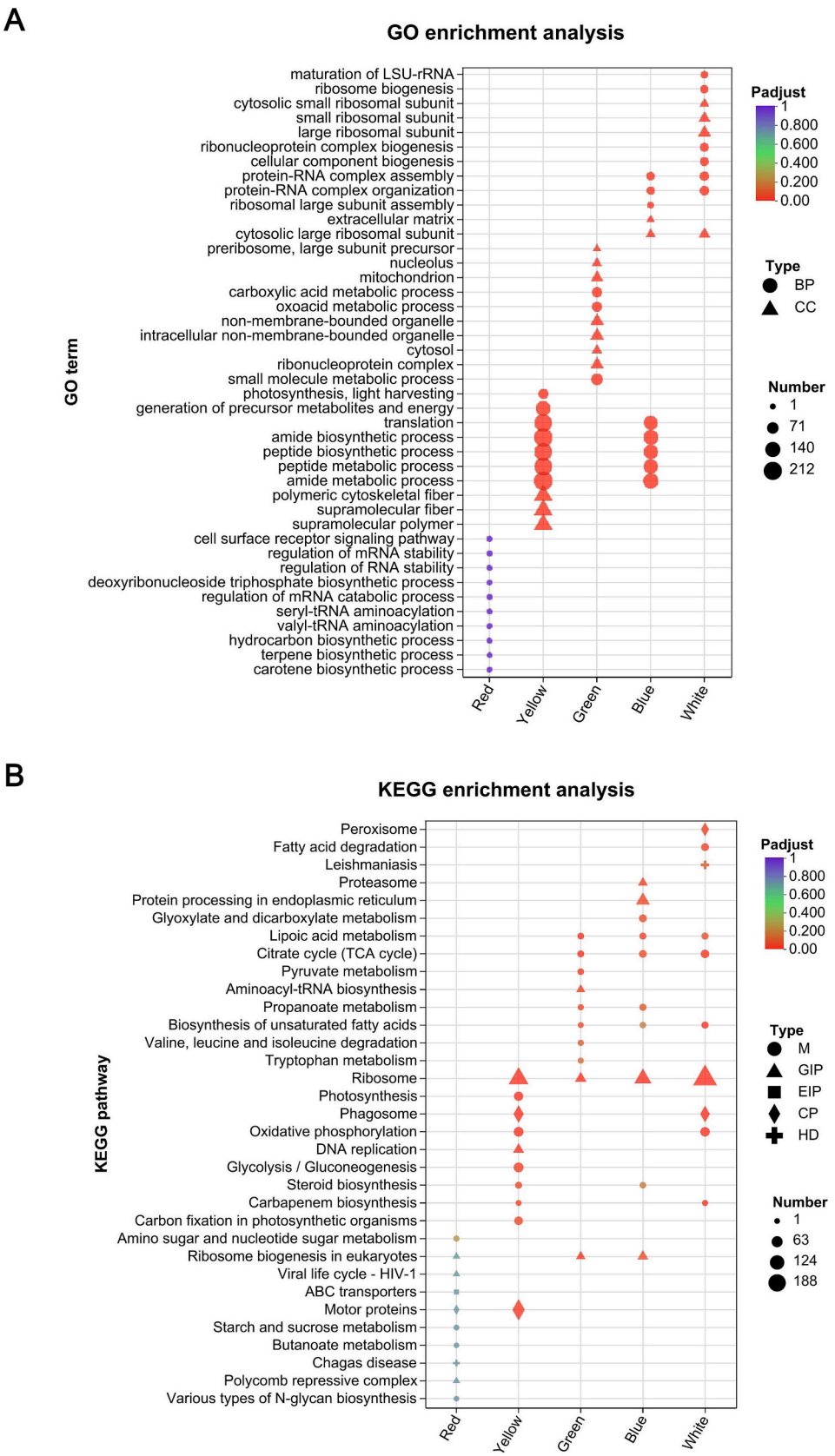

Fig. 6. Functional enrichment analysis of DEGs in each group after exposure to PS-MPs. (A) Bubble chart of multi-gene set GO enrichment analysis. (B) Bubble chart of multi-gene set KEGG enrichment analysis. Three biological replicates.

impaired growth and energy synthesis. This energy limitation was further exacerbated by PS-MPs-induced downregulation of key metabolic pathways, as demonstrated by transcriptomic data showing suppressed DEGs in lipoic acid metabolism, unsaturated fatty acid biosynthesis, and TCA cycle-all essential for energy transduction (Zhao et al., 2023; Cheng et al., 2024). Functional annotation revealed severe macromolecular metabolic deficiencies in blue and white groups, particularly in nitrogen/phosphorus assimilation, correlating with their maximal growth inhibition. Specifically, the combined effects of inhibited fatty acid degradation in white groups and disrupted protein processing in blue groups created synergistic bottlenecks in both energy supply and anabolic capacity, explaining their pronounced growth suppression (Zheng et al., 2025). Moreover, the color variations of plastic products in the environment often result from manufacturers using different types of dyes. In this sense, the distinct effects of these dyes on *Symbiodiniaceae* may be considered one of the factors contributing to the observed differences in the toxicity of microplastics of different colors. This is because microplastics of varying colors are unlikely to incorporate dyes with identical chemical compositions. In this study, all differently colored PS-MPs were obtained from the same manufacturer and product line, with identical particle size and polymer grade. Based on the supplier's specifications and previous studies (e.g., Chen et al., 2020), we assumed in our experimental design that these PS-MPs were consistent in material composition and additives, differing only in color. However, as FTIR or Raman spectroscopy was not performed in this work to directly verify this assumption, a degree of uncertainty remains. Future studies should employ spectroscopic characterization to further confirm the chemical consistency of differently colored PS-MPs.

4.2. Regulatory mechanisms for photosynthetic homeostasis in *C. goreaui* under PS-MPs exposure

EPS production constitutes an adaptive strategy in algae, where environmentally induced secretion of these polysaccharide-protein complexes mediates both proliferation and stress defense (Li et al., 2020). However, excessive EPS promotes aggregation with MPs, causing color-dependent shading that attenuates light availability and alters transcription of photosynthesis-related genes, as demonstrated by 1 μm PS-MPs forming dense EPS-MP complexes on *Chlorella pyrenoidosa* surfaces that critically impair light-harvesting capacity (Cao et al., 2022b). Under light-limiting conditions, the algal cells upregulated chlorophyll biosynthesis to enhance photosynthetic efficiency, thereby maintaining photostasis (Falkowski and Owens, 1980). The *Symbiodiniaceae* within corals transition from a monolayer to a multilayer configuration during winter months with lower temperature and light intensity to enhance light capture efficiency, whereas under summer conditions of elevated temperature and irradiance, both their density and photosynthetic pigment content decrease (Venn et al., 2008). These seasonal adaptations demonstrate the algal symbionts' capacity to modulate their photopigmentation to maintain photosynthetic homeostasis. In this study, the red and blue PS-MPs treatment groups exhibited a significant increase in photosynthetic pigment content compared to the control, while *Fv/fm* values remained unchanged. This indicates that, despite color-dependent shading and aggregation stress, *C. goreaui* maintained photosynthetic performance via compensatory upregulation of pigment-synthesis genes, consistent with transcriptomic evidence. Similarly, Su et al. (2020) reported that chl-a content in *C. goreaui* significantly increased on day 7 following exposure to 1 μm PS-MPs at a concentration of 5 mg/L, while photochemical efficiency remained unchanged throughout the exposure period. However, due to the necessity of counteracting toxic and/or oxidative stress, the photosynthetically derived energy was largely diverted from growth-related processes. This pattern may reflect the limited light availability caused by the poor reflectivity of white PS-MPs, which constrained photosynthetic input and ultimately led to pigment reduction. Moreover, spectral differences among coral reef substrates have been reported to influence light absorption and, consequently, chlorophyll content in *Symbiodiniaceae* (Xu et al., 2019). In this study, the significant differences in photosynthetic pigment content across treatment groups may be explained by the distinct spectral absorption and reflection characteristics of the surface dyes on PS-MPs, which likely altered the wavelengths of light reaching algal cells. Although the majority of differentially expressed genes related to photosynthesis and light-harvesting were downregulated in the yellow group, photosynthetic pigment levels and *Fv/fm* remained largely unaffected. This phenomenon may be attributed to the efficient absorption of yellow light by *C. goreaui*, likely owing to the spectral similarity between the yellow PS-MPs and the intrinsic pigmentation of the algal cells.

4.3. Defensive mechanisms and oxidative damage of *C. goreaui* following exposure to PS-MPs

Higher EPS content leads to increased attachment of particulate matter, enhancing co-aggregation and further elevating EPS levels, which in turn causes severe oxidative damage to the cells (Chen et al., 2012). The higher the EPS content, the more severe the cellular exposure to toxic substances, resulting in greater oxidative damage to the cells. Soluble proteins, as key nutrients and osmotic regulators, enhance cellular water retention and protect vital cellular components and biological membranes, making them commonly used as indicators for screening cellular resistance (Guzmán-Murillo et al., 2007; Qian et al., 2008). Our investigation showed that EPS and soluble protein levels in the red, blue, and white groups increased significantly, with higher increases compared to the yellow and green groups. These color-dependent increases suggest that greater aggregation and shading by chromatically mismatched PS-MPs enhance stress signaling, consistent with transcriptomic activation of EPS and stress-response genes.

Algal cells possess mechanisms for both the production and removal of reactive oxygen species (ROS), maintaining a dynamic equilibrium. However, excessive ROS, including superoxide radicals (O^{2-}), hydroxyl radicals (•OH), and hydrogen peroxide (H_2O_2), are generated upon exposure to toxic pollutants (Cao et al., 2022a; Jin et al., 2024). When ROS cause severe damage to the cell membrane and organelles, cells activate their immune system to produce antioxidant enzymes such as CAT, SOD, and POD to mitigate the negative effects of ROS (Cao et al., 2015). In the present work, SOD activity significantly increased in all experimental groups, with the red, blue, and white groups showing greater increases than the yellow and green groups. This pattern reflects higher ROS production induced by color-dependent aggregation and shading, consistent with transcriptomic activation of oxidative stress pathways.

MDA, a product of membrane lipid peroxidation, serves as an indicator of oxidative damage in algal cells. Excessive ROS promotes lipid peroxidation of the cell membrane, thereby increasing MDA levels (Qian et al., 2008; Cao et al., 2022a; Cao et al., 2022b). All experimental groups showed a significant increase in MDA levels, indicating that PS-MPs exposure causes severe oxidative damage to *C. goreaui*. The red, blue, and white groups, which exhibit greater color differences from the algal cells, generated higher ROS levels and exhibited higher MDA content, resulting in more extensive cellular damage. Carotenoids, as antioxidants in living organisms, play a crucial role in scavenging lipid peroxidation free radicals, and the increase in carotenoid levels is closely linked to the cellular capacity to eliminate reactive oxygen species (Kaur et al., 2024; Sanniyasi et al., 2024). Following PS-MPs exposure, carotenoid content significantly increased in all groups except the yellow group, suggesting a compensatory defense response coordinated with transcriptional regulation of antioxidant pathways. The decline in functions related to cytosolic large ribosomal subunits, protein-RNA complex assembly, and protein-RNA complex organization in the blue and white groups, as observed in transcriptomic results, could be one of the key reasons for the severe cellular damage in these

groups. The reduction in ribosomal function slows down metabolic processes, leading to severe ROS accumulation, while the impaired function of protein receptors responsible for antioxidant enzyme production prevents timely ROS clearance, exacerbating cellular damage. Moreover, the downregulation of peroxisomal pathways in the white group weakens its ability to eliminate ROS, resulting in the most severe lipid peroxidation, which may explain the highest MDA levels observed in this group.

4.4. Ecological implications: Symbiosis disruption and coral reef risk assessment

The symbiotic relationship between reef-building corals and *Symbiodiniaceae* underpins the ecological stability and productivity of coral reef ecosystems (Matthews et al., 2020). *Symbiodiniaceae* supply up to 90 % of the energy required by their coral hosts through photosynthetic carbon translocation (Ros et al., 2020). Our findings reveal that MPs exposure, particularly from blue and white PS-MPs, induces severe physiological stress, oxidative damage, and metabolic suppression in *C. goreaui*, which could reduce its contribution to the host's energy budget. The enhanced immune response of symbiotic algae to their host also induces metabolic trade-offs, deplete energy reserves and consequently reduces photoprotective capacity (Tang et al., 2025). Through quantitative analytical reasoning, if algal photosynthate translocation decreases by ~90 %, key coral functions such as calcification (potentially reduced by 50–70 %), protein synthesis (reduced by ~40 %), reproduction (reduced by 30–50 %), and stress resilience (reduced thermal tolerance by 1–2 °C) are likely to be compromised (Dufault et al., 2013; Schoepf et al., 2013; Hughes et al., 2018). Impaired algal function compromises the translocation of essential photosynthates to corals, reducing host energy reserves and exacerbating susceptibility to bleaching and mortality under environmental stress (Suggett et al., 2017). Moreover, previous studies have shown that oxidative imbalance and metabolic reprogramming in *Symbiodiniaceae* are key early events preceding symbiosis breakdown (Wang et al., 2020). Therefore, the physiological impairments observed in this study could initiate or intensify coral bleaching phenomena, particularly under combined stressors such as warming or eutrophication.

It should be noted that the experimental MP concentrations used here (20 mg/L) are higher than the typical background levels in coral reef waters (~0.1–10 mg/L), but fall within reported hotspots of local pollution (John et al., 2022; Yu and Singh, 2023). This comparison suggests that even moderate environmental MPs may pose cumulative risks to algal symbionts and consequently the coral energy supply. Given the increasing ubiquity of MPs in coral reef habitats (Ding et al., 2019a; Kaandorp et al., 2023; Lin et al., 2024), our results underscore the urgent need to incorporate MP-induced symbiosis disruption into coral reef health assessments and risk models. This study provides critical mechanistic evidence linking MP pollution to coral-algal symbiosis destabilization, offering a novel dimension to the ecological risk framework for coral reefs. Future conservation strategies should thus prioritize mitigating MP contamination alongside addressing climate-induced stressors to safeguard reef ecosystem resilience.

5. Conclusion

This study shows that PS-MP toxicity to *C. goreaui* is strongly color-dependent, with blue and white particles—most divergent from algal pigmentation—causing the greatest physiological and molecular disruptions. Although photosynthesis was maintained via increased pigment content, much energy was diverted to counter oxidative stress, impairing growth and cellular homeostasis. Transcriptomic analysis revealed suppression of genes in key biosynthetic, metabolic, and energy pathways, especially fatty acid metabolism and ribosomal function. These findings shed light on the mechanisms by which microplastics compromise the health of *Symbiodiniaceae*, potentially destabilizing coral-algal mutualisms and reef resilience, highlighting the urgent need to mitigate MP contamination.

CRediT authorship contribution statement

Tianyi Niu: Writing – review & editing, Writing – original draft, Visualization, Validation, Software, Methodology, Investigation, Formal analysis, Data curation, Conceptualization. **Yating Yang:** Writing – review & editing, Validation, Software, Investigation. **Sanqiang Gong:** Writing – review & editing, Supervision, Methodology, Formal analysis, Conceptualization. **Kefu Yu:** Supervision, Resources, Project administration, Funding acquisition, Data curation. **Jiayuan Liang:** Writing – review & editing, Supervision, Resources, Project administration, Methodology, Funding acquisition, Formal analysis, Data curation, Conceptualization.

Declaration of competing interest

The authors declare that they have no known competing financial interests or personal relationships that could have appeared to influence the work reported in this paper.

Acknowledgements

This work was supported by the National Natural Science Foundation of China (42030502 and 42090041), the Self-Topic Project of Guangxi Laboratory on the Study of Coral Reefs in the South China Sea (GXLSCRSCS2023101), and the Science and Technology Project of Guangxi (Nos. AD17129063 and AA17204074).

Appendix A. Supplementary data

Supplementary data to this article can be found online at https://doi.org/10.1016/j.marpolbul.2025.118815.

Data availability

The data generated as part of this study are available upon request. The raw sequence data (a total of 18 RNA sequencing libraries) produced in this study were deposited in the Sequence Read Archive (PRJNA1255781) of the NCBI (https://www.ncbi.nlm.nih.gov/bioproject/PRJNA1255781).

References

Auta, H., Emenike, C., Fauziah, S., 2017. Screening of *Bacillus* strains isolated from mangrove ecosystems in peninsular Malaysia for microplastic degradation. Environ. Pollut. 231, 1552–1559.

Baker, D.M., Andras, J.P., Jordán-Garza, A.G., Fogel, M.L., 2013. Nitrate competition in a coral symbiosis varies with temperature among *Symbiodinium* clades. ISME J. 7 (6), 1248–1251.

Cao, D.-j., Shi, X.-d., Li, H., Xie, P.-p., Zhang, H.-m., Deng, J.-w., Liang, Y.-G., 2015. Effects of lead on tolerance, bioaccumulation, and antioxidative defense system of green algae, Cladophora. Ecotoxicol. Environ. Saf. 112, 231–237.

Cao, Q., Jiang, Y., Yang, H., Zhang, Y., Wei, W., 2022a. Comprehensive toxic effects of povidone iodine on microalgae Chlorella pyrenoidosa under different concentrations. Aquac. Res. 53 (5), 1833–1841.

Cao, Q., Sun, W., Yang, T., Zhu, Z., Jiang, Y., Hu, W., Wei, W., Zhang, Y., Yang, H., 2022b. The toxic effects of polystyrene microplastics on freshwater algae Chlorella pyrenoidosa depends on the different size of polystyrene microplastics. Chemosphere 308, 136135.

Chen, P., Powell, B.A., Mortimer, M., Ke, P.C., 2012. Adaptive interactions between zinc oxide nanoparticles and Chlorella sp. Environ. Sci. Technol. 46 (21), 12178–12185.

Chen, Q., Li, Y., Li, B., 2020. Is color a matter of concern during microplastic exposure to Scenedesmus obliquus and Daphnia magna? J. Hazard. Mater. 383, 121224.

Cheng, S., Keang, K., Cross, J.S., 2024. Evidence that microplastics at environmentally relevant concentration and size interfere with energy metabolism of microalgal community. J. Hazard. Mater. 476, 134995.

Croce, R., Van Amerongen, H., 2014. Natural strategies for photosynthetic light harvesting. Nat. Chem. Biol. 10 (7), 492–501.

Ding, J., Jiang, F., Li, J., Wang, Z., Sun, C., Wang, Z., Fu, L., Ding, N.X., He, C., 2019a. Microplastics in the coral reef systems from Xisha Islands of South China Sea. Environ. Sci. Technol. 53 (14), 8036–8046.
Ding, J., Li, J., Sun, C., Jiang, F., Ju, P., Qu, L., Zheng, Y., He, C., 2019b. Detection of microplastics in local marine organisms using a multi-technology system. Anal. Methods 11 (1), 78–87.
Dufault, A.M., Ninokawa, A., Bramanti, L., Cumbo, V.R., Fan, T.-Y., Edmunds, P.J., 2013. The role of light in mediating the effects of ocean acidification on coral calcification. J. Exp. Biol. 216 (9), 1570–1577.
Falkowski, P.G., Owens, T.G., 1980. Light—shade adaptation: two strategies in marine phytoplankton. Plant Physiol. 66 (4), 592–595.
Fisher, R., O'Leary, R.A., Low-Choy, S., Mengersen, K., Knowlton, N., Brainard, R.E., Caley, M.J., 2015. Species richness on coral reefs and the pursuit of convergent global estimates. Curr. Biol. 25 (4), 500–505.
Ford, P.W., Garshott, D.M., Narasimhan, M., Ge, X., Jordahl, E.M., Subramanya, S., Bennett, E.J., 2025. RNF10 and RIOK3 facilitate 40S ribosomal subunit degradation upon 60S biogenesis disruption or amino acid starvation. Cell Rep. 44 (3).
González-Pech, R.A., Bhattacharya, D., Ragan, M.A., Chan, C.X., 2019. Genome evolution of coral reef symbionts as intracellular residents. Trends Ecol. Evol. 34 (9), 799–806.
Greenway, J.A., Gerstenberger, S., 2010. An evaluation of lead contamination in plastic toys collected from day care centers in the Las Vegas Valley, Nevada, USA. Bull. Environ. Contam. Toxicol. 85, 363–366.
Guibert, I., 2024. Assisted evolution of algal symbionts to enhance coral reef bleaching tolerance: a success story. Glob. Chang. Biol. 30 (1), e17150.
Guillard, R., Hargraves, P., 1993. Stichochrysis immobilis is a diatom, not a chrysophyte. Phycologia 32 (3), 234–236.
Guzmán-Murillo, M.A., López-Bolaños, C.C., Ledesma-Verdejo, T., Roldan-Libenson, G., Cadena-Roa, M.A., Ascencio, F., 2007. Effects of fertilizer-based culture media on the production of exocellular polysaccharides and cellular superoxide dismutase by Phaeodactylum tricornutum (Bohlin). J. Appl. Phycol. 19, 33–41.
Han, C., Shi, C., Liu, L., Han, J., Yang, Q., Wang, Y., Li, X., Fu, W., Gao, H., Huang, H., 2024. Majorbio cloud 2024: update single-cell and multiomics workflows. Imeta 3 (4), e217.
Horie, Y., Mitsunaga, K., Yamaji, K., Hirokawa, S., Uaciquete, D., Ríos, J., Yap, C., Okamura, H., 2024. Variability in microplastic color preference and intake among selected marine and freshwater fish and crustaceans. Discov. Oceans. 1, 5.
Houlbrèque, F., Ferrier-Pagès, C., 2009. Heterotrophy in tropical scleractinian corals. Biol. Rev. 84 (1), 1–17.
Huang, Y., Yan, M., Xu, K., Nie, H., Gong, H., Wang, J., 2019. Distribution characteristics of microplastics in Zhubi reef from South China Sea. Environ. Pollut. 255, 113133.
Hughes, T.P., Baird, A.H., Bellwood, D.R., Card, M., Connolly, S.R., Folke, C., Grosberg, R., Hoegh-Guldberg, O., Jackson, J.B., Kleypas, J., 2003. Climate change, human impacts, and the resilience of coral reefs. science 301 (5635), 929–933.
Hughes, T.P., Kerry, J.T., Baird, A.H., Connolly, S.R., Dietzel, A., Eakin, C.M., Heron, S. F., Hoey, A.S., Hoogenboom, M.O., Liu, G., 2018. Global warming transforms coral reef assemblages. Nature 556 (7702), 492–496.
Jambeck, J.R., Geyer, R., Wilcox, C., Siegler, T.R., Perryman, M., Andrady, A., Narayan, R., Law, K.L., 2015. Plastic waste inputs from land into the ocean. Science 347 (6223), 768–771.
Jiang, S., Lu, H., Xie, Y., Zhou, T., Dai, Z., Sun, R., He, L., Li, C., 2025. Toxicity of microplastics and nano-plastics to coral-symbiotic alga (Dinophyceae Symbiodinium): evidence from alga physiology, ultrastructure. OJIP kinetics and multi-omics. Water Research 273, 123002.
Jin, W., Zhang, W., Tang, H., Wang, P., Zhang, Y., Liu, S., Qiu, J., Chen, H., Wang, L., Wang, R., 2024. Microplastics exposure causes the senescence of human lung epithelial cells and mouse lungs by inducing ROS signaling. Environ. Int. 185, 108489.
John, J., Nandhini, A., Velayudhaperumal Chellam, P., Sillanpää, M., 2022. Microplastics in mangroves and coral reef ecosystems: a review. Environ. Chem. Lett. 20 (1), 397–416.
Jones, L.A., Mannion, P.D., Farnsworth, A., Bragg, F., Lunt, D.J., 2022. Climatic and tectonic drivers shaped the tropical distribution of coral reefs. Nat. Commun. 13 (1), 3120.
Kaandorp, M., Lobelle, D., Kehl, C., Dijkstra, H., Van Sebille, E., 2023. Global mass of buoyant marine plastics dominated by large long-lived debris. Nat. Geosci. 16, 689–694.
Karpestam, E., Merilaita, S., Forsman, A., 2014. Natural levels of colour polymorphism reduce performance of visual predators searching for camouflaged prey. Biol. J. Linn. Soc. 112 (3), 546–555.
Kaur, J., Khan, S., Taleuzzaman, M., 2024. Carotenoids' neuroprotective effects via a free radical scavenging pathway, and they are being characterized, and evaluated as food additives. In: Microbial Vitamins and Carotenoids in Food Biotechnology. Elsevier, pp. 401–426.
Kazancı, Y., Alyürük, N., Alpergün, C., Kara, N., Baycan, N., Gündüz, O., 2025. Analysis of microplastic flux from the Gediz River to the Aegean Sea: a modeling study for environmental management. J. Environ. Manag. 391, 126412.
Kühn, S., Van Franeker, J.A., 2020. Quantitative overview of marine debris ingested by marine megafauna. Mar. Pollut. Bull. 151, 110858.
Lagarde, F., Olivier, O., Zanella, M., Daniel, P., Hiard, S., Caruso, A., 2016. Microplastic interactions with freshwater microalgae: hetero-aggregation and changes in plastic density appear strongly dependent on polymer type. Environ. Pollut. 215, 331–339.
Lambert, S., Sinclair, C.J., Bradley, E.L., Boxall, A.B., 2013. Effects of environmental conditions on latex degradation in aquatic systems. Sci. Total Environ. 447, 225–234.
Li, C., Wang, X., Liu, K., Zhu, L., Wei, N., Zong, C., Li, D., 2021a. Pelagic microplastics in surface water of the eastern Indian Ocean during monsoon transition period: abundance, distribution, and characteristics. Sci. Total Environ. 755, 142629.
Li, J., Ouyang, Z., Liu, P., Zhao, X., Wu, R., Zhang, C., Lin, C., Li, Y., Guo, X., 2021b. Distribution and characteristics of microplastics in the basin of Chishui River in Renhuai, China. Sci. Total Environ. 773, 145591.
Li, S., Wang, P., Zhang, C., Zhou, X., Yin, Z., Hu, T., Hu, D., Liu, C., Zhu, L., 2020. Influence of polystyrene microplastics on the growth, photosynthetic efficiency and aggregation of freshwater microalgae Chlamydomonas reinhardtii. Sci. Total Environ. 714, 136767.
Liang, J., Niu, T., Zhang, L., Yang, Y., Li, Z., Liang, Z., Yu, K., Gong, S., 2025. Polystyrene microplastics exhibit toxic effects on the widespread coral symbiotic Cladocopium goreaui. Environ. Res. 268, 120750.
Lin, J., Zhao, Y.-M., Zhan, Z.-G., Zheng, J.-Y., Zhou, Q.-Z., Peng, J., Li, Y., Xiao, X., Wang, J.-H., 2024. Microplastics in remote coral reef environments of the Xisha Islands in the South China Sea: source, accumulation and potential risk. J. Hazard. Mater. 469, 133872.
Liu, D., Guo, Z.-F., Xu, Y.-Y., Chan, F.K.S., Xu, Y.-Y., Johnson, M., Zhu, Y.-G., 2022. Widespread occurrence of microplastics in marine bays with diverse drivers and environmental risk. Environ. Int. 168, 107483.
Lu, H., Ni, Z., Wang, Y., Ye, S., 2025. Deposition characteristics of microplastics in coral reef fish with different feeding habits from the Xisha Islands waters, South China Sea. J. Environ. Manag. 378, 124736.
Matthews, J.L., Raina, J.B., Kahlke, T., Seymour, J.R., van Oppen, M.J., Suggett, D.J., 2020. Symbiodiniaceae-bacteria interactions: rethinking metabolite exchange in reef-building corals as multi-partner metabolic networks. Environ. Microbiol. 22 (5), 1675–1687.
Mellin, C., Brown, S., Cantin, N., Klein-Salas, E., Mouillot, D., Heron, S.F., Fordham, D.A., 2024. Cumulative risk of future bleaching for the world's coral reefs. Science. Advances 10 (26), eadn9660.
Ni, C., Buszczak, M., 2023. The homeostatic regulation of ribosome biogenesis. In: Seminars in cell & developmental biology. Elsevier, pp. 13–26.
Peixoto, R.S., Sweet, M., Bourne, D.G., 2019. Customized medicine for corals. Frontiers Media SA.
Peters, C.A., Thomas, P.A., Rieper, K.B., Bratton, S.P., 2017. Foraging preferences influence microplastic ingestion by six marine fish species from the Texas Gulf Coast. Mar. Pollut. Bull. 124 (1), 82–88.
Pogoreutz, C., Voolstra, C.R., Rädecker, N., Weis, V., Cardenas, A., Raina, J.-B., 2020. The coral holobiont highlights the dependence of cnidarian animal hosts on their associated microbes. In: Cellular Dialogues in the Holobiont. CRC Press, pp. 91–118.
Qian, H., Chen, W., Sheng, G.D., Xu, X., Liu, W., Fu, Z., 2008. Effects of glufosinate on antioxidant enzymes, subcellular structure, and gene expression in the unicellular green alga Chlorella vulgaris. Aquat. Toxicol. 88 (4), 301–307.
Qin, L., Xu, Y., Chen, J., Niu, T., Yu, K., Liang, J., 2023. Optimization of in vitro culture method for zooxanthellae associated with reef-building corals. Acta Microbiol Sin. 63 (04), 1658–1671. https://doi.org/10.13343/j.cnki.wsxb.20220656.
Reaka-Kudla, M.L., 1997. The global biodiversity of coral reefs: a comparison with rain forests. Biodiversity II: Understanding and protecting our biological resources 2, 551.
Ritchie, R.J., 2006. Consistent sets of spectrophotometric chlorophyll equations for acetone, methanol and ethanol solvents. Photosynth. Res. 89, 27–41.
Ros, M., Camp, E.F., Hughes, D.J., Crosswell, J.R., Warner, M.E., Leggat, W.P., Suggett, D.J., 2020. Unlocking the black-box of inorganic carbon-uptake and utilization strategies among coral endosymbionts (Symbiodiniaceae). Limnol. Oceanogr. 65 (8), 1747–1763.
Sanniyasi, E., Gopal, R.K., Raj, P.P., Kalaiselvi, R., Chandhinipriya, S., 2024. Extraction, characterization and the antioxidant activity of carotenoid pigment canthaxanthin from an aero-terrestrial and filamentous green microalga Trentepohlia sp. Bioresource Technology Reports 25, 101803.
Schoepf, V., Grottoli, A.G., Warner, M.E., Cai, W.-J., Melman, T.F., Hoadley, K.D., Pettay, D.T., Hu, X., Li, Q., Xu, H., 2013. Coral energy reserves and calcification in a high-CO2 world at two temperatures. PLoS One 8 (10), e75049.
Schreiber, U., Schliwa, U., Bilger, W., 1986. Continuous recording of photochemical and non-photochemical chlorophyll fluorescence quenching with a new type of modulation fluorometer. Photosynth. Res. 10, 51–62.
Sendra, M., Pereiro, P., Yeste, M.P., Mercado, L., Figueras, A., Novoa, B., 2021. Size matters: zebrafish (Danio rerio) as a model to study toxicity of nanoplastics from cells to the whole organism. Environ. Pollut. 268, 115769.
Shaw, D.G., Day, R.H., 1994. Colour-and form-dependent loss of plastic micro-debris from the North Pacific Ocean. Mar. Pollut. Bull. 28 (1), 39–43.
Shtykova, L., Ostrovskii, D., Jacobsson, P., Nydén, M., 2006. Interaction between medetomidine and alkyd resins: NMR and FTIR investigation of antifouling marine paint model systems. J. Appl. Polym. Sci. 99 (5), 2797–2809.
Smith, S., 1978. Coral-reef area and the contributions of reefs to processes and resources of the world's oceans. Nature 273 (5659), 225–226.
Su, L., Xue, Y., Li, L., Yang, D., Kolandhasamy, P., Li, D., Shi, H., 2016. Microplastics in taihu lake, China. Environ. Pollut. 216, 711–719.
Su, Y., Zhang, K., Zhou, Z., Wang, J., Yang, X., Tang, J., Li, H., Lin, S., 2020. Microplastic exposure represses the growth of endosymbiotic dinoflagellate Cladocopium goreaui in culture through affecting its apoptosis and metabolism. Chemosphere 244, 125485.
Suggett, D.J., Warner, M.E., Leggat, W., 2017. Symbiotic dinoflagellate functional diversity mediates coral survival under ecological crisis. Trends Ecol. Evol. 32 (10), 735–745.

Sun, Y., 2020. Studies on Physiological Response and Omics Analysis of Early Development of Tow Reff Corals to Ocean Warming and Acidification. University of Chinese Academy of Sciences, Doctor.
Tang, C.-H., Lin, C.-Y., Li, H.-H., 2025. Coral incorporating microplastics leads to a health-risking immunometabolic shift. Chemosphere 374, 144245.
Thompson, R.C., Olsen, Y., Mitchell, R.P., Davis, A., Rowland, S.J., John, A.W., McGonigle, D., Russell, A.E., 2004. Lost at sea: where is all the plastic? Science 304 (5672), 838.
Ursell, L.K., Metcalf, J.L., Parfrey, L.W., Knight, R., 2012. Defining the human microbiome. Nutr. Rev. 70 (suppl_1), S38–S44.
van Woesik, R., Kratochwill, C., 2022. A global coral-bleaching database, 1980–2020. Sci Data 9 (1), 20.
Venn, A.A., Loram, J.E., Douglas, A.E., 2008. Photosynthetic symbioses in animals. J. Exp. Bot. 59 (5), 1069–1080.
Wang, S., Chen, H., Zhou, X., Tian, Y., Lin, C., Wang, W., Zhou, K., Zhang, Y., Lin, H., 2020. Microplastic abundance, distribution and composition in the mid-West Pacific Ocean. Environ. Pollut. 264, 114125.
Wang, S., Feng, R., Hu, K., Hu, X., Qu, Q., Mu, L., Wen, J., Ma, C., 2024. Polystyrene microplastics facilitate formation of refractory dissolved organic matter and reduce CO2 emissions. Environ. Int. 190, 108809.
Wang, W., Ndungu, A.W., Li, Z., Wang, J., 2017. Microplastics pollution in inland freshwaters of China: a case study in urban surface waters of Wuhan, China. Sci. Total Environ. 575, 1369–1374.
Wang, Z., He, Y., Luo, M., Liu, S., Hou, J., Cao, B., An, X., 2025. Transfer toxicity of polystyrene microplastics in vivo: multi-organ crosstalk. Environ. Int. 109604.
Webster, N.S., Thomas, T., 2016. The sponge hologenome. MBio 7 (2). https://doi.org/10.1128/mbio. 00135-00116.
Wen, B., Liu, J.-H., Zhang, Y., Zhang, H.-R., Gao, J.-Z., Chen, Z.-Z., 2020. Community structure and functional diversity of the plastisphere in aquaculture waters: does plastic color matter? Sci. Total Environ. 740, 140082.
Woodhead, A.J., Hicks, C.C., Norström, A.V., Williams, G.J., Graham, N.A., 2019. Coral reef ecosystem services in the Anthropocene. Funct. Ecol. 33 (6), 1023–1034.
Wright, S.L., Thompson, R.C., Galloway, T.S., 2013. The physical impacts of microplastics on marine organisms: a review. Environ. Pollut. 178, 483–492.
Xia, F., Tan, Q., Qin, H., Wang, D., Cai, Y., Zhang, J., 2023. Sequestration and export of microplastics in urban river sediments. Environ. Int. 181, 108265.
Xu, J., Li, f., Meng, Q., Wang, F., 2019. The analysis of spectral Separability of different coral reef benthos and influence of pigments on coral spectra based on in situ data. Spectrosc. Spectr. Anal. 39 (08), 2462–2469.
Yu, K., 2018. Introduction to the Science of Coral Reefs, 1st ed. Science Press, Beijing.
Yu, R.-S., Singh, S., 2023. Microplastic pollution: threats and impacts on global marine ecosystems. Sustainability 15 (17), 13252.
Yue, F., Zhang, J., Xu, J., Niu, T., Lü, X., Liu, M., 2022. Effects of monosaccharide composition on quantitative analysis of total sugar content by phenol-sulfuric acid method. Front. Nutr. 9, 963318.
Zettler, E.R., Mincer, T.J., Amaral-Zettler, L.A., 2013. Life in the "plastisphere": microbial communities on plastic marine debris. Environ. Sci. Technol. 47 (13), 7137–7146.
Zhang, C., Chen, X., Wang, J., Tan, L., 2017. Toxic effects of microplastic on marine microalgae Skeletonema costatum: interactions between microplastic and algae. Environ. Pollut. 220, 1282–1288.
Zhang, J., Choi, C.E., Gao, F., 2024. Effects of microplastics on the rheological properties of sediment slurries in aquatic environments. Environ. Int. 193, 109095.
Zhang, K., Shi, H., Peng, J., Wang, Y., Xiong, X., Wu, C., Lam, P.K., 2018. Microplastic pollution in China's inland water systems: a review of findings, methods, characteristics, effects, and management. Sci. Total Environ. 630, 1641–1653.
Zhao, T., Tan, L., Han, X., Ma, X., Lin, K., Wang, J., 2023. Energy metabolism response induced by microplastic for marine dinoflagellate Karenia mikimotoi. Sci. Total Environ. 866, 161267.
Zhao, X., Wang, J., Yee Leung, K.M., Wu, F., 2022. Color: an important but overlooked factor for plastic photoaging and microplastic formation. Environ. Sci. Technol. 56 (13), 9161–9163.
Zheng, Y., Li, J., Zhu, H., Hu, J., Sun, Y., Xu, G., 2025. Endocytosis, endoplasmic reticulum, actin cytoskeleton affected in tilapia liver under polystyrene microplastics and BDE153 acute co-exposure. Comp. Biochem. Physiol., Part C: Toxicol. Pharmacol. 289, 110117.
Zhou, Z., Zhang, P., Zhang, G., Wang, S., Cai, Y., Wang, H., 2021. Vertical microplastic distribution in sediments of Fuhe River estuary to Baiyangdian wetland in northern China. Chemosphere 280, 130800.